Dear author,

Please note that changes made in the online proofing system will be added to the article before publication but are not reflected in this PDF.

We also ask that this file not be used for submitting corrections.

Q2 # Calcium carbonate fouling on double-pipe heat exchanger with different heat exchanging surfaces

Q3 K.H. Teng [a,b,*], S.N. Kazi [a,**], Ahmad Amiri [c,***], A.F. Habali [a], M.A. Bakar [a], B.T. Chew [a], A. Al-Shamma'a [b], A. Shaw [b], K.H. Solangi [d], Ghulamulah Khan [a]

[a] Department of Mechanical Engineering, University of Malaya, 50603 Kuala Lumpur, Malaysia
[b] Department of Built Environment, Liverpool John Moores University, Byron Street, Liverpool, L3 3AF, United Kingdom
[c] Department of Chemical Engineering, Faculty of Engineering, Ferdowsi University of Mashhad, Mashhad, Iran
[d] Department of Mechanical and Aerospace Engineering Missouri, University of Science and Technology, Rolla, 65409, MO, United States

ABSTRACT

An experimental setup of double pipe heat exchanger fouling test rig was built to investigate the mineral scale deposition on different heat exchanger pipe surfaces. Progressive fouling deposition on different material surfaces under the similar solution conditions were observed and analyzed. Measurable data on the progressive build-up of scale deposits, deposition rate, as well as the composition and crystal morphology of the deposits were studied after each experimental run by analyzing the deposited scale on the test pipes. In this research the artificial calcium carbonate deposit on different material surfaces is considered as it is one of the major constituents of the most scales found in heat exchanging equipment. Fouling on different smooth test pipes were investigated in the centrally located larger concentric pipe heat exchanger. Uniform flow condition near the pipe surface was maintained by constant flow rate throughout the system. The calcium carbonate deposition rates on five different metal surfaces (Stainless steel 316, brass, copper, aluminium and carbon steel) were investigated. The results illustrated an upward trend for fouling rate with time on the tested specimens. The deposition on the surfaces showed a linear growth with the enhancement of thermal conductivity of the metals. However, deposition on carbon steel metal surfaces did not follow the typical linear trend of thermal conductivity over deposition as its surface was altered by corrosion effects. In addition, temperature, velocity, and concentration effects on fouling deposition were investigated on the SS316 metal surface. It is noted that the fouling deposition increases with the increase of temperature and concentration due to enhanced deposition potential whereas reduces due to the increase of velocity which enhances shear stress.

© 2017 Elsevier B.V. All rights reserved.

1. Introduction

Q6

Fouling can be defined as the formation of unwanted deposits on the heat transfer surfaces that impede heat transfer and increase the resistance to the flow of working fluids over surfaces [1]. Heat exchangers are of important equipment for industrial processes as they handle a major portion of the total energy consumption [2]. Water is the most common working fluid which is used as a cooling medium in the heat transfer-based processes. It is also used as a process fluid and even as a solvent [3]. Many industries tend to locate where an easy access to water is available. Rivers, lakes, oceans, etc. are the major sources of water. However, water is an universal solvent, that dissolves most of the components when they come in contact such as Ca^{2+} and Mg^{2+} and other minerals on earth [4]. When this water borne minerals are exposed to different physical influences, such as heat transfer, friction and pressure change, they can revert back into natural solid stage against one another and always lead to the formation of deposits on the surfaces and cause fouling problems [5,6].

These fouling layers usually contain calcium carbonate, calcium sulphates, calcium silicate, etc. which possess commonly a very low thermal conductivity [7]. Hence, it can decrease the heat transfer rate, increase pressure fluctuations in heat exchangers and introduce an overall loss of industrial output [8,9]. Operating costs are further increased by frequent shutdowns for cleaning and corresponding usage of chemical detergents and sanitizers; which also increase the environmental impact [10,11]. Mineral scale deposits can produce major

* Corresponding author at: Department of Mechanical Engineering, Faculty of Engineering, University of Malaya, 50603 Kuala Lumpur, Malaysia.
** Corresponding author at: Department of Mechanical Engineering, Faculty of Engineering, University of Malaya, 50603 Kuala Lumpur, Malaysia.
*** Corresponding author.
E-mail addresses: alex_teng1989@hotmail.com, K.H.Teng@2016.ljmu.ac.uk
Q4 (K.H. Teng), salimnewaz@um.edu.my, salimnewaz@yahoo.com (S.N. Kazi),
Q5 ahm.amiri@gmail.com (A. Amiri).

operational problems from poorly treated process waters. Moreover, corrosion may be caused by these mineral deposits [12,13]. Fouling is the source of several problems in equipment, such as deterioration of performance and limiting useful operating life of equipment [14,15]. Therefore, studies of the industrial problems regarding this topic are fundamental for understanding the risks associated to the reuse of process and effluent waters [16].

Potential damages towards equipment caused by the formation of scale can be very costly if process water is not treated properly. Chemicals are commonly employed to treat the process water by industries. Total of 7.3 billion dollars worth chemicals per year in the U.S. released in to the air, dumped in streams and buried in landfills every year. Globally, 40% are purchased by industry for control of the scale in cooling towers, boilers and other heat transfer equipment. That represents more than 2 billion dollars of toxic waste which contribute to trillions of gallons of contaminated water discarded annually on the earth which belongs to all the population of the earth.

An environmentally-friendly approach is essential to overcome these fouling problems without the use of chemicals, where most are toxic and/or corrosive. To address this issue, some researches and development on fouling have progressed significantly over the period of last 15-years [17]. The fouling mechanisms are now described in terms of processes associated with the formation, transportation, deposition, and removal mechanism [18]. Major technical issues still remain before water fouling can be recognized as a solved problem [19]. At present, water fouling can be considered as a manageable problem, but at a high cost and usage of chemicals with hazardous influences on the environment [20].

In this research work, an automated experimental test rig was built for conducting experiments on the factors affecting fouling rate (different metal surfaces, temperature, velocity and concentration). Kazi et al. have reported the calcium sulphate deposition on different material surfaces under different circumstances [21]. The present research has focused on the study of deposition of artificially-hardened calcium carbonate in a double-pipe heat exchanger. This is important to simulate a real case of plant operational process related to the heat exchanger equipment since these two materials (calcium carbonate and calcium sulphate) are considered to be the major constituents of the most scale formed in such equipment [22,23].

2. Experimental

2.1. (i) Apparatus

The schematic diagram of the experimental apparatus is presented in Fig. 1. The apparatus consists of two flow loops with two separate tanks containing artificial fouling solution (blue line) and hot water (red line) respectively with a test section (Heat exchanger). The hot flow loop comprises of a frequency controlled magnetic gear pump, N-Flow 25 magnetic flow meter, pipes of different metal surfaces and a thermostatically controlled heater to maintain the heater tank at a constant hot inlet temperature (50 ± 0.5 °C). The hot line outside the test section is insulated thoroughly to prevent heat loss along the flowing line. Also, the cold flow loop contains a jacketed artificial fouling solution tank, frequency controlled magnetic gear pump, transparent HDPE piping for flowing line, Burkert inline paddle wheel flow meter, RW20 digital stirrer and a chiller to maintain the artificial fouling solution at a constant cold inlet temperature (25 ± 0.5 °C). The cold line magnetic gear pump (Araki Magnet Pump) has the specifications of 2800 rpm, 1.1 amps, 260 W motor and of capacity 120 L/min, with maximum head of 8.6 m.

The test section is a counter current double pipe heat exchanger with the length of 130 cm. In this exchanger, the hot water flows into the pipe and cold artificial fouling solution in the annular space of the pipe. The inside pipe is made of different metals with the same dimensions (outer diameter of 12.7 mm and inner diameter of 8.48 mm). The outer pipe is of transparent HDPE piping with the inner diameter (ID) of 42.1 mm and outer diameter (OD) of 46.8 mm.

The inlet and outlet temperatures in the hot and cold lines were measured using 4 RTD sensors. A PLC program data acquisition system was installed for collecting data and automatically maintaining hot and cold inlet sections at the specified temperatures. The pressure drop variation in both the lines across the test section was measured using YOKOGAWA Differential Pressure Transmitter (0–200 mbar). During the fouling test, the volume flow rate, pressure drop, inlet and outlet temperatures for hot and cold lines were recorded.

2.2. (ii) Test specimens

The experimental pipes are 1300 mm in length with a wall thickness of 2.11 mm and outer diameter of 12.7 mm. Five metal pipes (copper, aluminium, brass, carbon steel and stainless steel 316) with the same dimensions were used in these experiments. The test section pipes and the coupons of the same materials were connected by precise machining of the inner and the outer threads as the connector. As it can be seen in Fig. 2, the coupons were installed in the middle of test section. Characterizations of the fouling deposition on the surfaces were conducted after completion of the fouling tests.
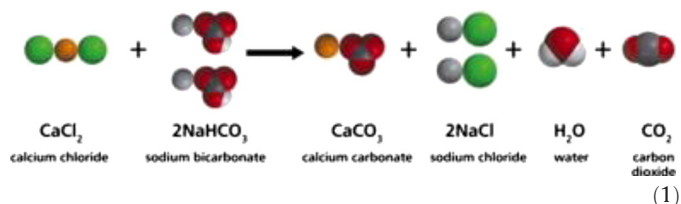
The smooth test specimens piping's (Table 1) were used in the as-received condition but before installing in the test rig, they were cleaned by rubbing with a water-soaked cloth and flushing with hot water to remove any deposition of grease, oil, etc.

2.3. (iii) Data acquisition

A programmable logic controller (PLC) was installed and a software WinCC was employed to record the inlet and outlet temperatures of hot water passing through the pipe, the mean temperature of tanks, inlet and outlet of artificial solution temperatures passing through the annular pipe, differential pressure between annular pipe and flow rates of hot line and solution line. All the temperatures were measured using the RTD-100 sensors. Also, the differential pressure and flow rates were recorded by a transmitting 4–20 mA signal via PLC to the software. The program was set in recoding mode of every 10 min interval and continuous up to 4320 min [24].

2.4. (iv) Experimental procedures

Fouling rate, fouling resistances and total deposition formed on different heat exchanger surfaces by varying parameters were conducted by using fouling test experiment. Leakage test was performed prior to the experimental runs to ensure the suitability and validity of the setup and working conditions. The experimental setup was cleaned by circulating distilled water and also using chemical cleaning agents (Decon 90) before each experimental run to ensure reproducibility of data. To accelerate the scaling effect in a short period of time, artificial fouling solution containing 300 mg/l $CaCO_3$ was prepared using proportionate amount of calcium chloride ($CaCl_2$) and sodium bicarbonate ($NaHCO_3$) in distilled water. Eq. (1) illustrates the calcium carbonate formation from the reaction between calcium chloride and sodium bicarbonate in water [25].

| $CaCl_2$ | $2NaHCO_3$ | $CaCO_3$ | $2NaCl$ | H_2O | CO_2 |
| calcium chloride | sodium bicarbonate | calcium carbonate | sodium chloride | water | carbon dioxide |

(1)

The flow of the artificial fouling solution was varied from 0.15 to 0.45 m/s and the flow of the hot water through the inner tube
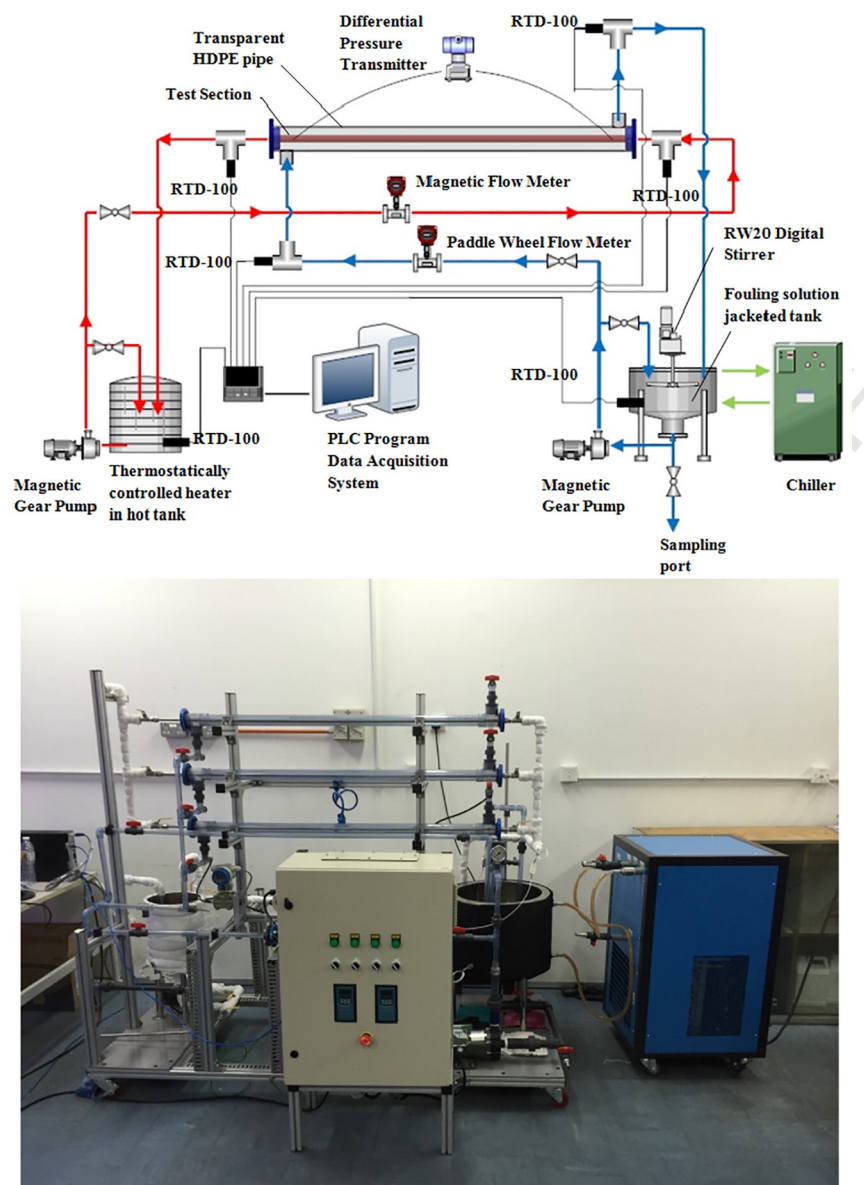
Fig. 1. Double pipe heat exchanger experimental test rig.

was maintained constant at 1 m/s. The inlet temperatures of the hot and cold flows were set at constant values of 50 $\pm$ 0.5 °C and 25 $\pm$ 0.5 °C respectively. The solution hardness was maintained at a constant value of 300 $\pm$ 30 mg/L throughout the experiments and the hardness of the solutions were measured by EDTA complexometric titration method. The stirrer in the solution
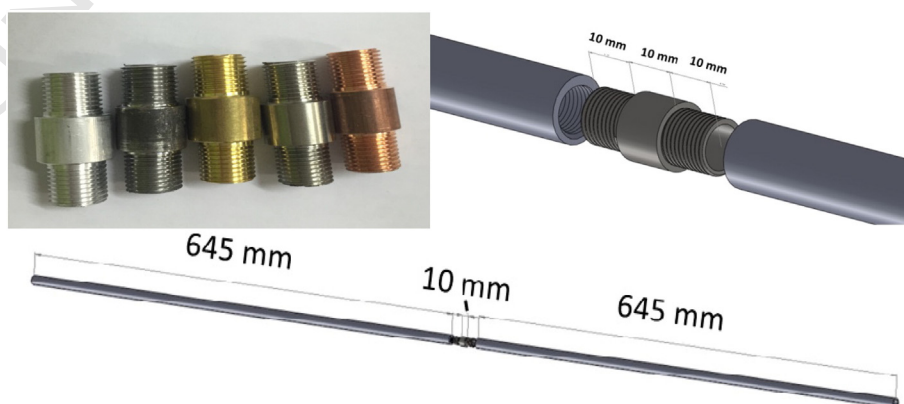

Fig. 2. Coupons installation of different materials on heat exchanger surfaces.

Materials	Properties at 300 K			
	p (kg/m³)	C_p (J/kg·K)	K (W/m·K)	R_a (μm)
Stainless steel	8238	468	16	1.27
Carbon steel	7850	502	90	2.34
Brass	8530	380	109	2.18
Aluminium	2702	903	250	2.16
Copper	8960	385	401	2.22

Fig. 4. Reproducibility of the experimental run results under same conditions.

tank was operated at 475 rpm to ensure homogeneity of the artificial fouling solution.

As a common correlation, Eq. (2) was used to calculate the fouling resistance, R_f, throughout the experimental tests and to monitor fouling behaviour on the surface of metal.

$$R_f = \frac{1}{U_{fouled}} - \frac{1}{U_{initial}} \quad (2)$$

Where, U_{fouled} and $U_{initial}$ are the overall heat transfer coefficient for the fouled case and the overall heat transfer coefficient for the initial clean condition, respectively. These overall heat transfer coefficients were calculated by using the Eq. (3).

$$Q = UA\Delta T_{LMTD} \quad (3)$$

Where, Q is the thermal energy of heat transfer section, U is the overall heat transfer coefficient, $A = 2\pi RL$, is the total surface area of the heat transfer section and ΔT_{LMTD} (Eq. (4)) is the log mean temperature difference, which was determined from the measured temperatures at the inlet and outlet of hot and solution water:

$$\Delta T_{LMTD} = \frac{(T_{h,out} - T_{c,in}) - (T_{h,in} - T_{c,out})}{\ln\left[\frac{(T_{h,out} - T_{c,in})}{(T_{h,in} - T_{c,out})}\right]} \quad (4)$$

2.5. (v) Measurement and characterization

The amount of deposition has been determined by dissolving the deposited scale in diluted HCl solution and later applied complexometric titration by EDTA. After 72 h fouling test run, the test section pipe was dismantled carefully (without any damage to the deposited scale) from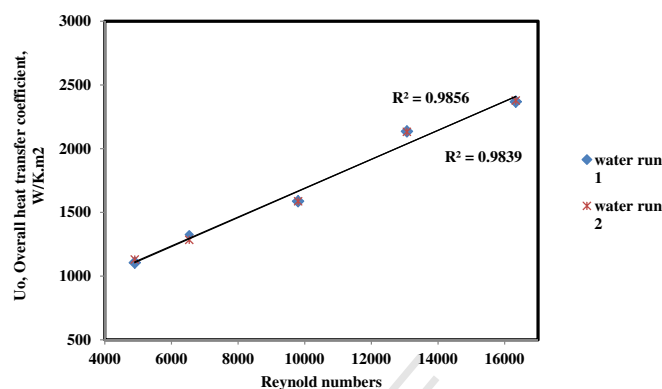 the heat exchanger. Then the calcium carbonate deposited on the test section surface was extracted using diluted HCl solution. Soft brush was used to clean the surface and then the solution was collected into a beaker and diluted into 1 L using distilled water and the amount of calcium carbonate deposition was determined using EDTA-complexometric titration method. The coupons were carefully removed earlier from the test pipe for characterization of the deposits. The polymorphic composition and crystal morphology of the scale deposits were characterized by x-ray diffraction analysis (XRD) and scanning electron microscopy (SEM) respectively. In addition, the elemental analysis was checked by energy dispersive spectroscopy (EDS). Optical images and photographs were obtained to visually differentiate the fouling deposition on different tested surfaces [26].
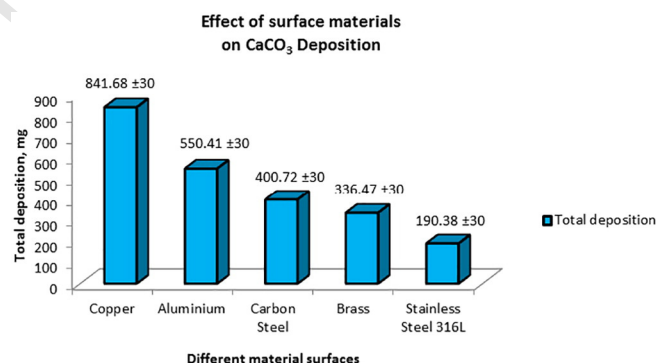

Fig. 5. Total depositions on different heat exchanger materials at 50 °C and 25 °C at hot and cold water inlet respectively, 0.15 m/s solution flow and 300 mg/l concentration.
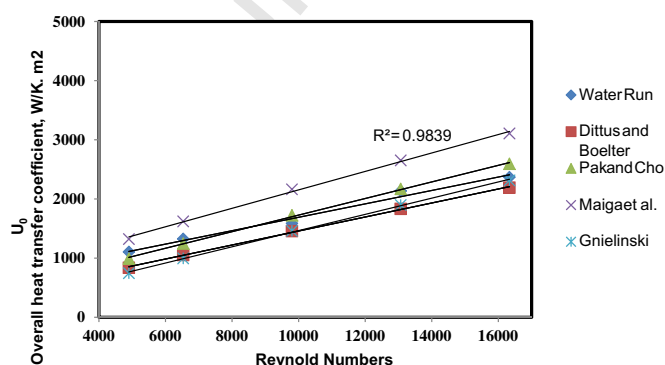

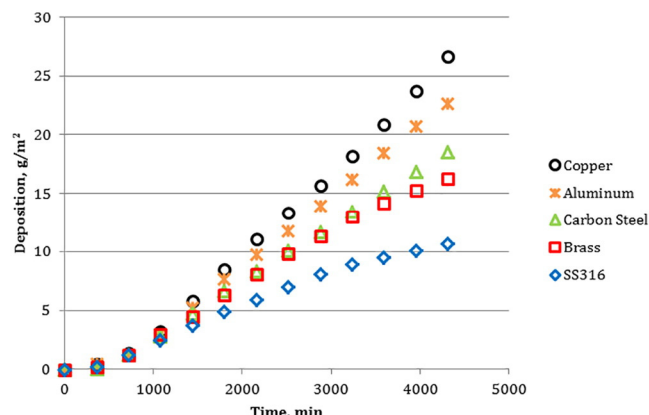**Fig. 3.** Validation of the experimental run results with standard equations.

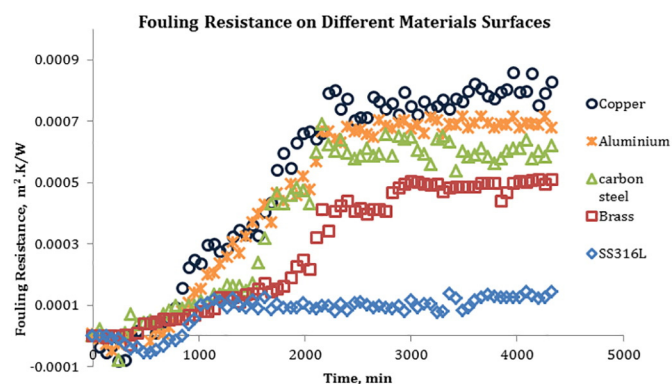**Fig. 6.** Deposition rate as the function of time on different heat exchanger materials.

Fig. 7. Fouling resistances as the function of time based on different heat exchanger materials at 50 °C and 25 °C at hot and solution inlet respectively, 0.15 m/s solution flow velocity and 300 mg/l concentration.

3. Results and discussion

3.1. (i) Data validation and reproducibility

Fig. 3 illustrates the validation of the experimental results by correlating with the following equations:

Maiga et al. [27] (Eq. (5))

$$Nu = 0.085 \ Re^{0.71} \ Pr^{0.35} \tag{5}$$

Dittus and Boelter [28] (Eq. (6))

$$Nu = 0.023 \ Re^{0.8} \ Pr^{0.4} \tag{6}$$

Pak and Cho [29] (Eq. (7))

$$Nu = 0.021 \ Re^{0.8} \ Pr^{0.5} \tag{7}$$

Gnielinkski equation [30] (Eq. (8))

$$Nu = \frac{\left(\frac{f}{8}\right)(Re-1000) \ Pr}{1 + 12.7 \left(\frac{f}{8}\right)^{0.5} \left(Pr^{\frac{2}{3}}-1\right)} \tag{8}$$

Where the friction factor is

$$f = (0.78 \ \ln \ Re - 1.64)^{-2}$$

The data was also reproduced and the results showed that there is a good agreement between two similar runs as seen in Fig. 4. The current setup shows that the current experimental test rig yielded a promising result for conducting fouling tests.

3.2. (ii) Fouling on various surface materials

The effect of these metals' nature (copper, aluminium, carbon steel, brass and stainless steel 316) on the deposition of calcium carbonate
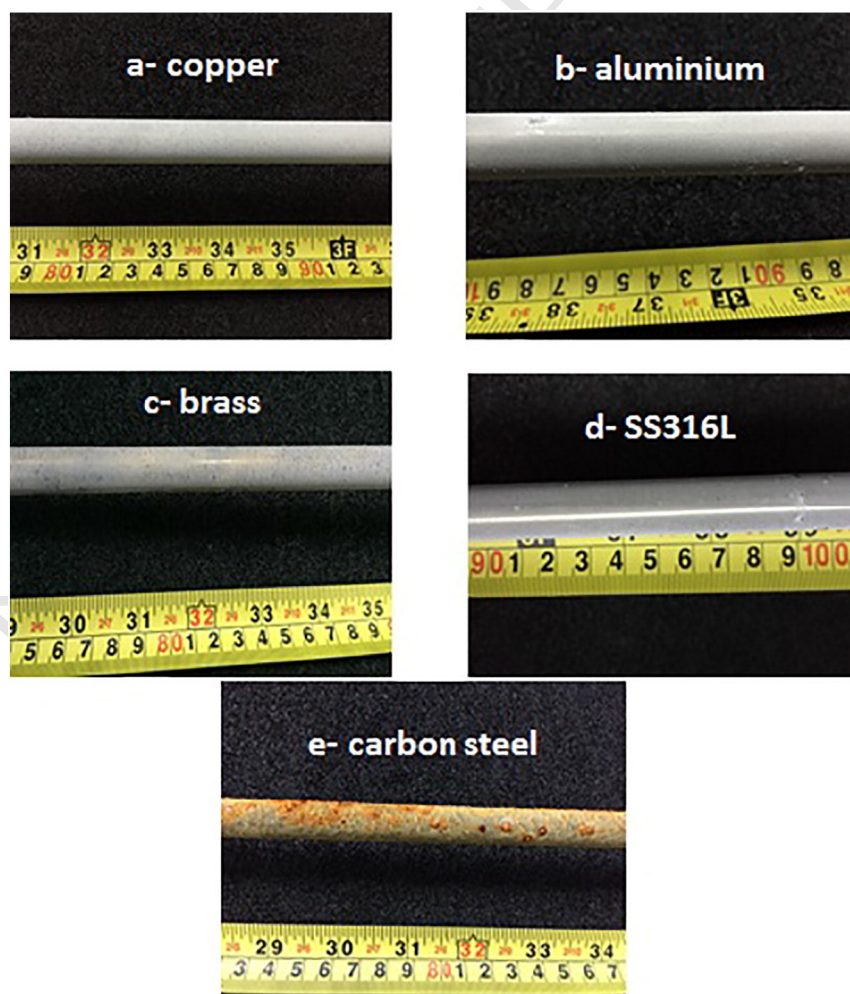

Fig. 8. Images of calcium carbonate deposition on different metal surfaces.
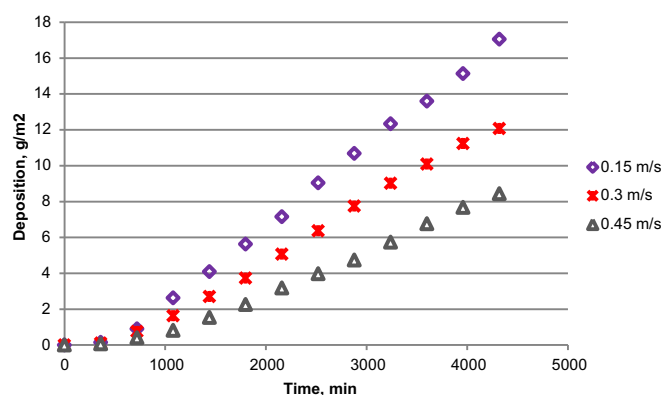
Fig. 9. Calcium carbonate depositions as the function of time under different velocity conditions on SS316L, 50 °C hot water inlet, 25 °C solution inlet and 300 mg/l concentration.

Fig. 11. Fouling resistance of deposition on SS316L under effect of hot inlet temperature at 25 °C solution inlet, 0.15 m/s solution flow velocity and 300 mg/l concentration.

253 scale was studied in a series of experiments [31,32]. The total deposi-
254 tions after fouling test on different heat exchanger metal surfaces are
255 shown in Fig. 5. It can be seen that copper and stainless steel-316
256 show the greatest and lowest quantities of deposition, constituting
257 841.68 and 190.38 mg, respectively.
258   It can be seen in Fig. 6, the depositions of calcium carbonate on five
259 different heat exchanger surfaces are in the sequence of; copper > alu-
260 minium > carbon steel > brass > stainless steel. Fig. 7 illustrates the foul-
261 ing resistance under the effect of different materials. It can be observed
262 that the deposition tends to be asymptotic which is consistent with pipe
263 flow investigations for all the materials. Kazi et al. obtained similar re-
264 sults for the deposition of calcium sulphate on different heat exchanger
265 materials which were consistent with the values of their thermal con-
266 ductivities [21].
267   The effect of various heat exchanger surface materials on surface de-
268 position has been mentioned in several studies [33,34] in which the de-
269 position on substrates was consistent with their thermal conductivity
270 values, i.e. copper > aluminium > brass > stainless steel. The experimen-
271 tal results appear to correlate well with thermal conductivity for copper,
272 aluminium, brass and stainless steel, which implies the increase in the
273 deposition with thermal conductivity enhancement.
274   Moreover, this research indicates that the carbon steel material did
275 not follow the thermal conductivity trends where it is expected to
276 yield lower fouling deposition compared to brass. As seen in Fig. 7, the
277 fouling resistance of carbon steel material at about 1500 min is dramat-
278 ically increased and overstep the fouling resistance of brass and moved
279 nearer to the aluminium. Severe corrosion was observed on the carbon
280 steel and due to this the deposition on carbon steel metal surfaces has
281 altered due to the corrosion effects (promoted by the rough surfaces).
282 Fig. 8 (a–e) shows the crystallization deposition on the different

283 materials at 0.15 m/s. It is obvious from Fig. 8 (e) that the corrosion foul-
284 ing is severe on carbon steel.

3.3. (iii) Fouling under effect of velocity

286   Fig. 9 illustrates the effect of flow velocity (between 0.15 and
287 0.45 m/s) on the fouling deposition rate. It is obvious from Fig. 9, that
288 the $CaCO_3$ deposition rate is inversely proportionate to velocity. Several
289 researchers have reported the similar results [35,36]. This could be

Fig. 12. Fouling resistance of deposition on SS316L under effect of concentration at 50 °C and 25 °C at hot and solution inlet respectively and 0.15 m/s solution flow velocity.
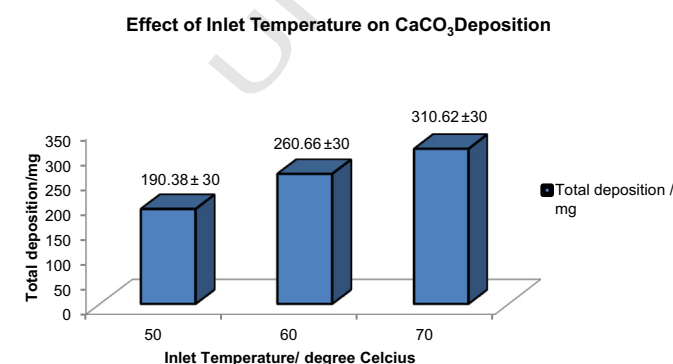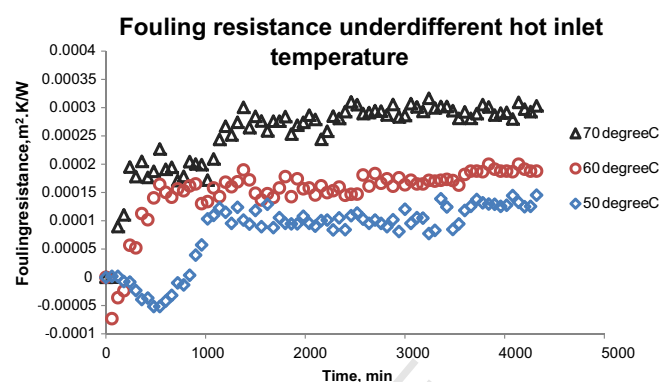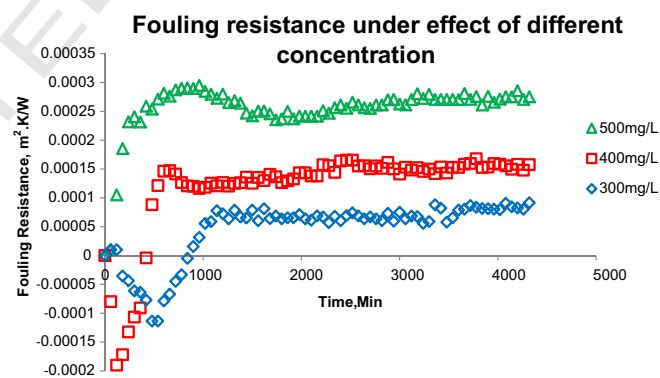

Fig. 10. Total depositions on SS316L under effect of temperature, at 25 °C solution inlet, 0.15 m/s solution flow velocity and 300 mg/l concentration.
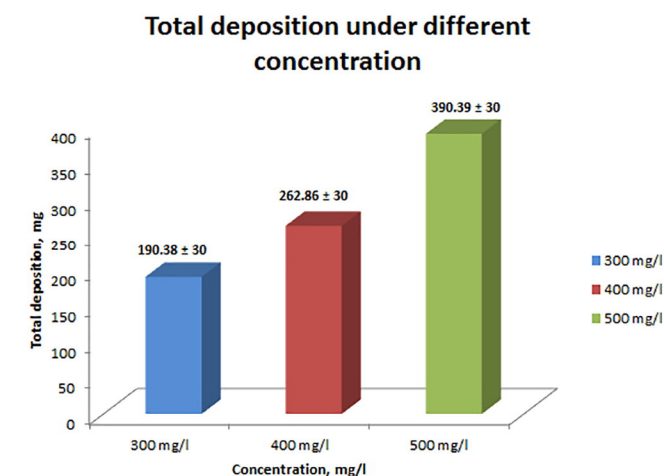

Fig. 13. Total depositions on SS316L under effect of concentration, at 50 °C and 25 °C at hot and solution inlet respectively and 0.15 m/s solution flow velocity.
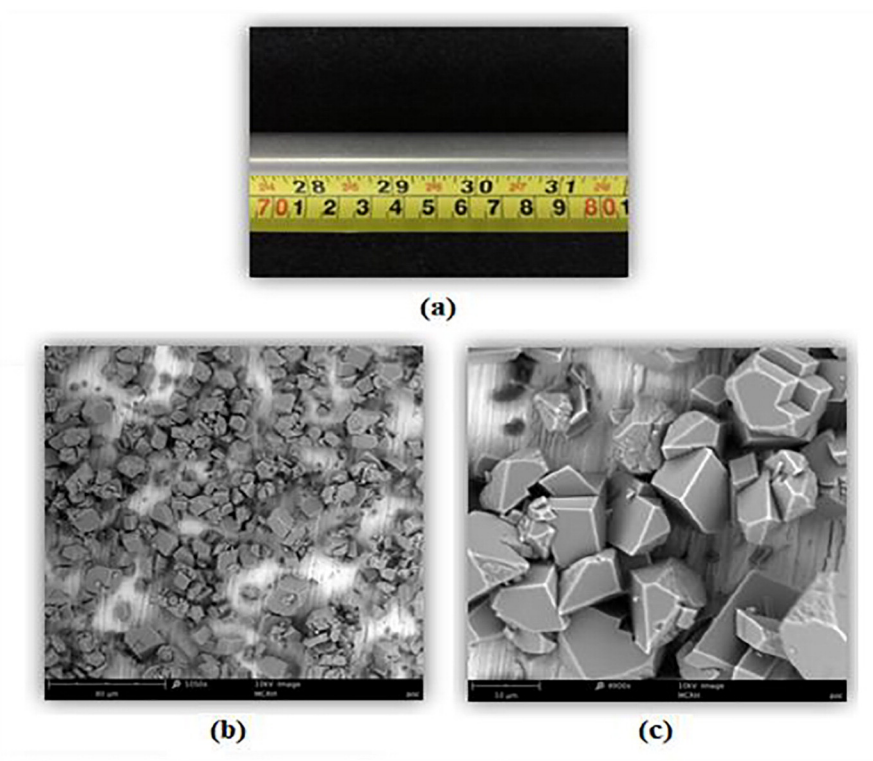
Fig. 14. Image (a) and crystal morphology (b & c) of calcium carbonate formation at 300 mg/l, 50 °C and 25 °C at hot and solution inlet respectively and 0.15 m/s solution flow velocity.

attributed to the significant removal of scale particles from the fouling deposition formation at higher velocities due to increased shear stress near the boundary wall of metal surfaces at the liquid-solid interface [37–39].

3.4. (iv) Fouling under effect of hot inlet temperature

Fouling under the effect of inlet temperature was conducted on stainless steel 316L at the constant velocity of 0.15 m/s. Calcium
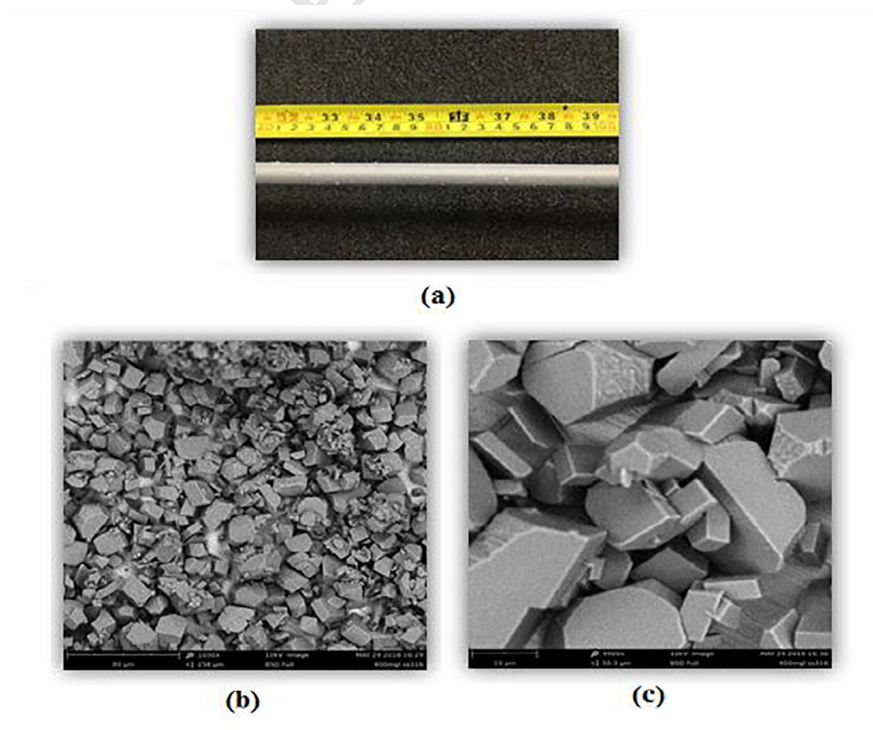

Fig. 15. Image (a) and crystal morphology (b & c) of calcium carbonate formation at 400 mg/l, 50 °C and 25 °C at hot and solution inlet respectively and 0.15 m/s solution flow velocity.

Fig. 16. Image (a) and crystal morphology (b & c) of calcium carbonate formation at 500 mg/l, 50 °C and 25 °C at hot and solution inlet respectively and 0.15 m/s solution flow velocity.
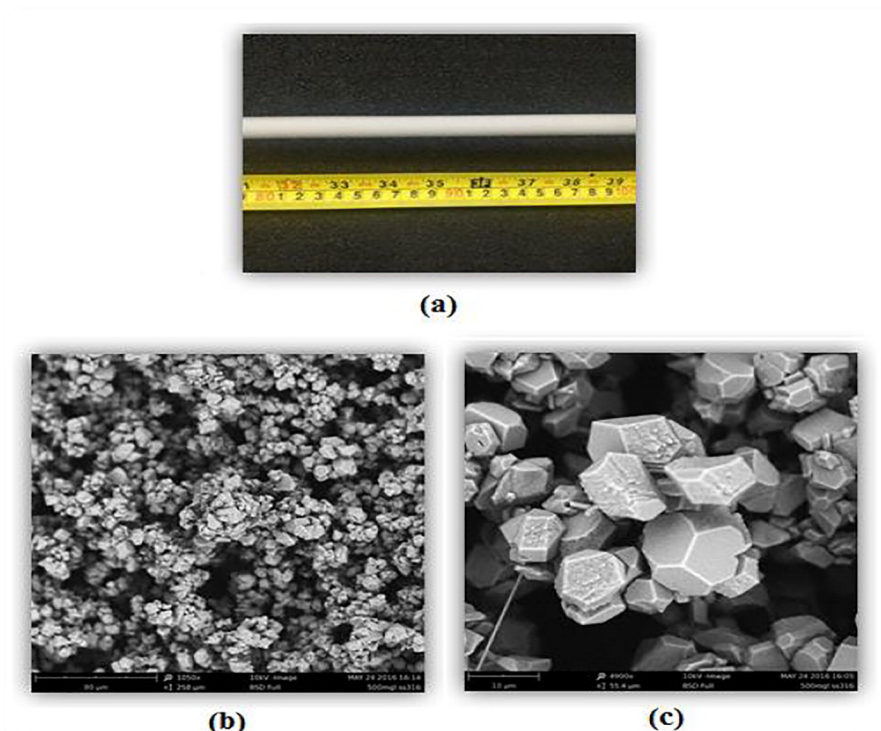
carbonate is an inversely soluble salt against temperature. Hence, it can be predicted that the composition of calcium carbonate scale deposits can be influenced by varying temperature [40,41]. As it can be seen in Fig. 10, higher inlet temperature induces higher total deposition on the SS316 material. In addition, longer induction period of scale formation at 50 °C in comparison to that at 70 °C was reported in Fig. 11. It indicates that the induction period of fouling depends strongly on the temperature. Similar results were reported by Mullin [42] where he

expressed the relationship between induction period and temperature in Eq. (9).

$$\log\left(T_{int}^{-1}\right) = A - \frac{E_a}{2.303RT} \tag{9}$$

Where, E_a is the molar activation energy for nucleation (J/mol), R is the universal gas constant, which is 8.3145 J/K.mol and A is a constant value.

3.5. (v) Fouling under effect of concentration

The effect of fouling solution hardness concentration was conducted in this double pipe heat exchanger and details are depicted in Figure 12. Kazi et al. reported that high concentration of calcium sulphate has significant impact on deposition of different materials [43]. It was observed (Fig. 12) that shortest induction period of less than one hour was
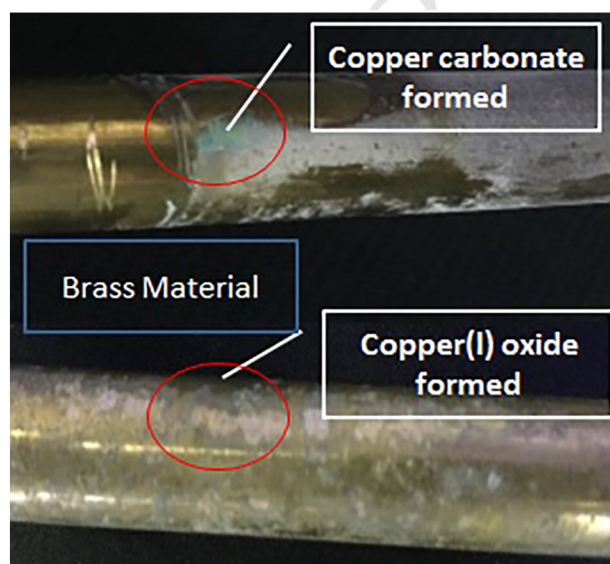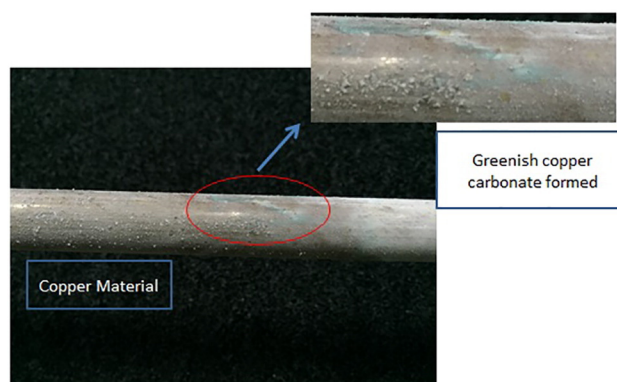

Fig. 17. Deposition on brass material.

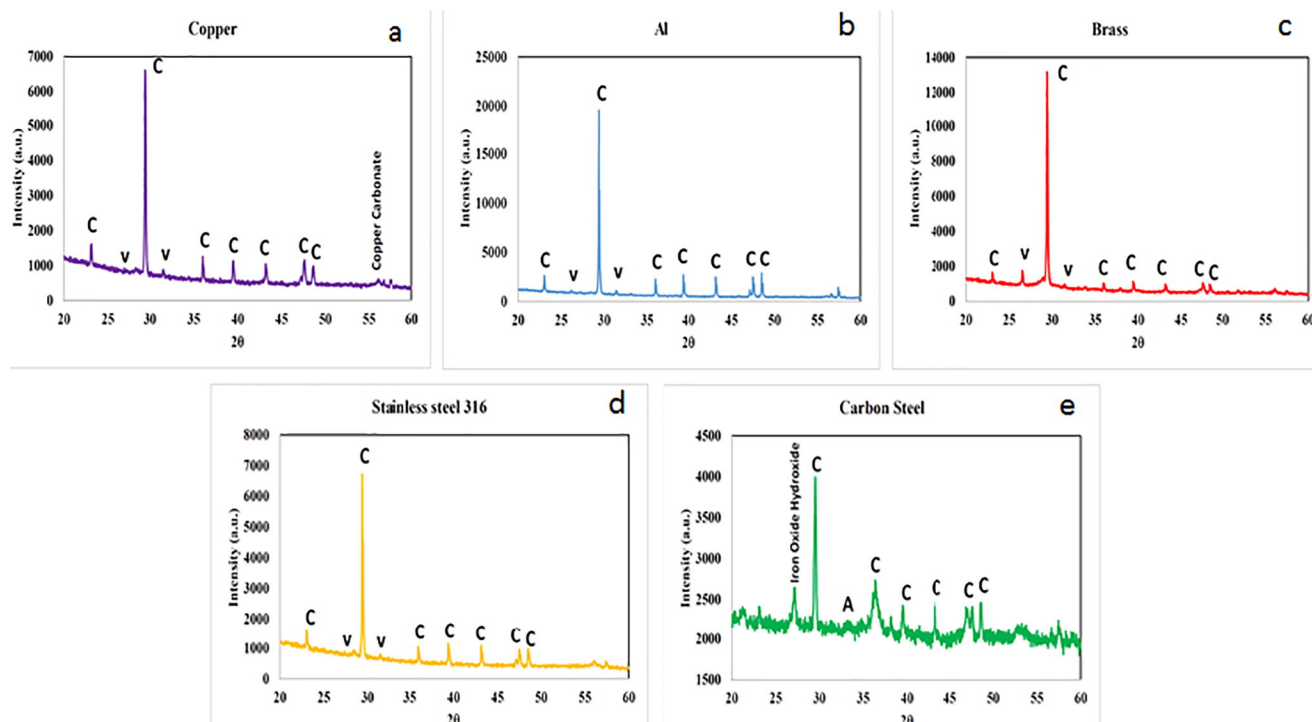**Fig. 18.** Deposition on copper material.

Fig. 19. XRD analyses of the deposited materials.

experienced to form scale layer at 500 mg/l concentration while 400 and 300 mg/l concentration it took 7 h and 14 h respectively. 500 mg/l showed highest fouling resistance resulting lowest heat transfer rate in the system. This shows that the scale deposition layer formed quickly at higher concentration compared to lower concentrations and indicates that the induction period of fouling depends strongly on concentration. Similarly, the amount of $CaCO_3$ deposited on SS 316 L at different fouling solution concentration is presented in Fig. 13. It showed
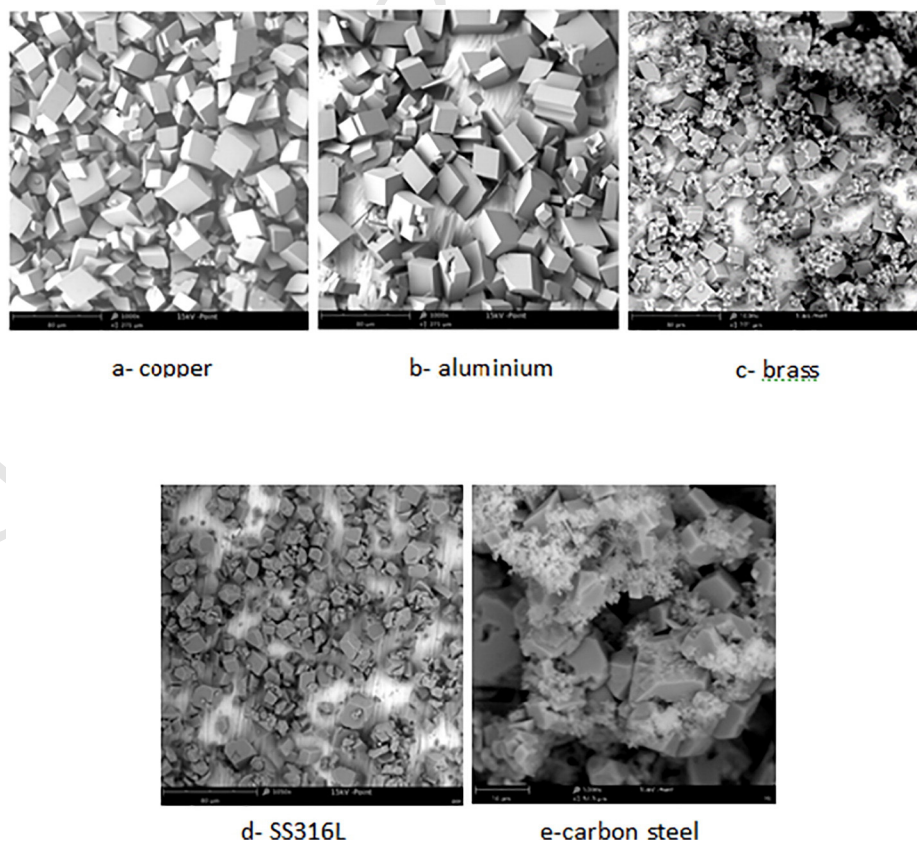

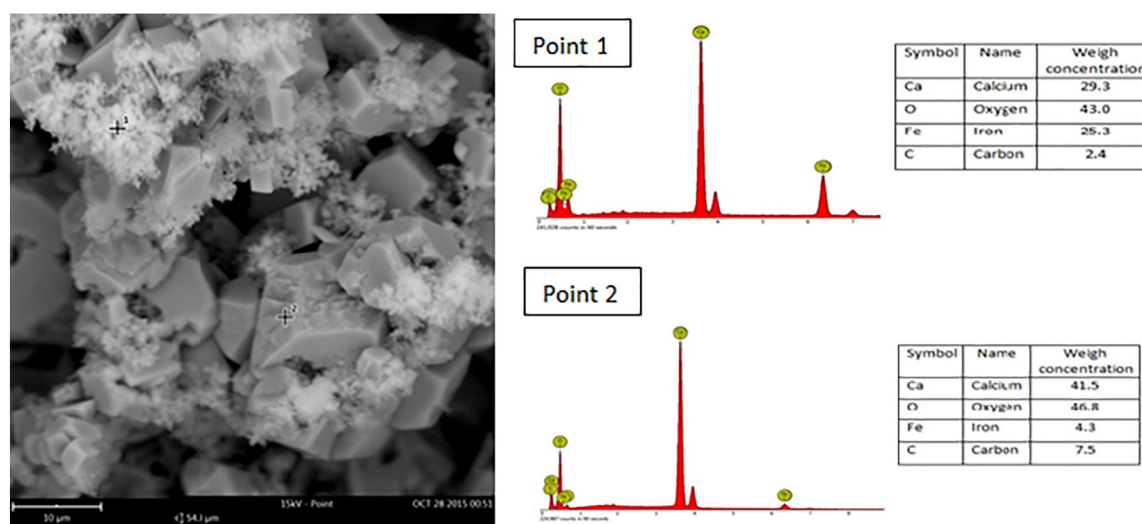**Fig. 20.** SEM analyses of the deposited materials.

Fig. 21. SEM and EDS analyses of the deposited materials on carbon steel.

that the amount of deposition is more than double when the concentration is increased from 300 mg/l to 500 mg/l. This is because at high concentration, the supersaturation is attained quickly and the circulating solution inside heat exchanger provides high nucleation rate and calcium carbonate precipitation from solution which eventually deposits on the metal surface.

The morphology of the samples was analyzed using scanning electron microscopes (SEM). As seen in Figs. 14 & 15, at concentration of 300 mg/l and 400 mg/l, crystalline of calcite which has sharp cubic edge and orthorhombic crystal structure were observed. It can be seen clearly, the crystal morphology is relative smaller in size at 300 mg/l (about 15 μm) compared to about 25 μm in 400 mg/l. This crystal structure type enhances the structure to form a robust fouling layer. At 500 mg/l, the crystal structure is a bit different compared to the other samples. Fig. 16 shows the crystal morphology of calcium carbonate formed at temperatures of 50 °C and 25 °C for hot and solution inlet respectively at the constant solution flow velocity of 0.15 m/s. The morphological structure exhibits on the surfaces and look like rougher in nature (16 c). The amorphous $CaCO_3$ appear to be metastable and aggregate into larger spherical particles (about 45 μm).The crystals simultaneously grow larger and accumulate to form a fouling layer of $CaCO_3$. The blunt cubic edge will give the structure less robust compared to sharp cubic structure. From the SEM images it is clear that the deposition at 500 mg/l is a mixture of particulate and crystalline structures.

3.6. (vi) Visualization of the fouling test section and crystal morphology

Figs. 17 and 18 show the deposition on brass and copper materials respectively. Note that only white deposition formed and no corrosion effects were observed on SS316 and aluminium after the fouling test. However, the deposits formed on the brass surfaces have green and reddish stains along with white encrustation of calcium carbonate, which indicate that the chemical reaction took place and hence some chemical fouling have observed as seen in Fig. 17. Deposits formed on copper pipe surface observed similarly with the green layer along with white deposits as seen in Fig. 18. It has happened due to the effect of chemical fouling and crystallization. Similar results were reported by Kazi et al. on calcium sulphate deposition [44]. Moreover, carbon steel observed a severe corrosion after the fouling test. A combination of crystallization fouling and corrosion fouling was observed on the carbon steel surface. In a nutshell, it could be concluded that industrial cooling waters are corrosion contributor of heat exchanger surfaces where there are combinations of various effects on fouling.

The x-ray diffraction spectrum (XRD) of the deposited materials on copper, aluminium, brass, SS316, and carbon steel are presented in Fig. 19 (a-e). It can be seen that the characteristic peaks at $2\theta \sim 29.3°$, 23.1°, 36.1°, 39.4°, 47.5°, and 48.7° verified the presence of calcite in all the substrates [45]. Deposition on all the metal exhibited the presence of binary mixture containing calcite and vaterite and the lack of aragonite is obvious [46]. Insignificant peaks of vaterite were observed at $2\theta \sim 26.7°$ and 31.4° indicating that its presence is in negligible quantity. It is noteworthy that copper and carbon steel demonstrate an oxidation phase representing copper carbonate and Iron oxide hydroxide peaks, respectively. Also, due to high intensities of the peaks of the metal substrate, the $CaCO_3$ polymorphic peaks were subdued and it made identification difficult. We know that the metal intensities were five to six times stronger than the $CaCO_3$ peaks due to which some of the peaks were subdued and sometimes missed in Fig. 19. Overall, pure calcite elements were the dominant component deposited on the surface of different metals.

Fig. 20 (a–e) shows SEM images of calcium carbonate deposition on SS316, brass, aluminium and copper and also corrosion products with calcium carbonate fouling on carbon steel. It can be clearly seen that the size of the crystallites/crystal structure has followed the trends of amount of total deposition; copper (about 40 μm) > aluminium (about 37.33 μm) > brass (about 20.36 μm) > stainless steel 316 (about 15 μm).These results are supporting the theory of crystal structure size which could determine the fouling deposition rate on the surfaces [47]. On the other hand, SEM images of carbon steel shows the combination of calcite and the corrosion products.

Fig. 21 shows the energy dispersive spectroscopy (EDS) of the combination of corrosion fouling and crystallization fouling on carbon steel materials. The composition of iron oxide and the deposition of calcite layer in between the iron oxide are represented as Point 1 and Point 2.

4. Conclusion

In these experiments, several variable parameters (velocity, temperature, concentration and materials effect) were studied systematically. In summary, it is observed that the calcium carbonate deposition on the surfaces increase linearly with the thermal conductivity of the metal. However, deposition on carbon steel metal surfaces did not follow the linear trend as it has been altered by the corrosion effects. Temperature has a great effect on the total deposition as well as the induction period of fouling deposition formed on the metal surfaces. In addition, velocity plays a vital role in determining the fouling

deposition thickness. These findings could be good references to use in designing systems and heat exchangers with the enhanced performance and lifespan which are topics to be addressed in the future research.

Nomenclature

od	Inside pipe outer diameter (mm)
id	Inside pipe inner diameter (mm)
OD	External pipe outer diameter (mm)
ID	External pipe inner diameter (mm)
RTD	Resistance temperature detector
PLC	Programmable logic controller
W_s	Weights of the deposited scale (g)
W_f	Weights of the fouled coupon (g)
W_I	Weights of the initial coupon (g)
R_f	Fouling resistance ($m^2 \cdot K/W$)
U_{fouled}	Overall heat transfer coefficient for the fouled case ($W \cdot m^{-2} \cdot K^{-1}$)
$U_{initial}$	Overall heat transfer coefficient for the initial case ($W \cdot m^{-2} \cdot K^{-1}$)
Q	Rate of heat gain (W)
A	Total heat transfer surfaces (m^2)
ΔT_{LMTD}	Log mean temperature difference which was determined from the measured temperatures at the inlet and outlet of hot and solution water (K)
$T_{hot,in}$	Temperature at hot inlet (K)
$T_{hot,out}$	Temperature at hot outlet (K)
$T_{cold,in}$	Temperature at cold inlet (K)
$T_{cold,out}$	Temperature at cold outlet (K)
Nu	Nusselt number
Re	Reynolds number
Pr	Prandtl number
f	friction factors
EDTA	Ethylenediaminetetraacetic acid
R_a	Average surface roughness

Conflict of interests

The authors declare that there is no conflict of interest regarding the publication of this paper.

Acknowledgements

References

[1] H. MÜLler-Steinhagen, M.R. Malayeri, A.P. Watkinson, Fouling of heat exchangers-new approaches to solve an old problem, Heat Transfer Eng. 26 (1) (2005) 1–4.

[2] T. Kuppan, Heat Exchanger Design Handbook, vol. 126, Marcel Dekker, New York, 2000.

[3] M.-S. Hans, C4 Fouling of Heat Exchanger Surfaces, in VDI Heat Atlas, Springer, Berlin Heidelberg, 2010 79–104.

[4] M.F. Humphrey, Cooling tower water conditioning study, Ozone Sci. Eng. 3 (2) (1981) 109–119.

[5] J.W. Mullin, Crystallisation, fourth ed. Butterworth-Heineman, London,UK, 2001.

[6] S. Mozia, et al., Effect of process parameters on fouling and stability of MF/UF TiO$_2$ membranes in a photocatalytic membrane reactor, Sep. Purif. Technol. 142 (2015) 137–148.

[7] S.N. Kazi, G.G. Duffy, X.D. Chen, Fouling and fouling mitigation on heated metal **Q10** surfaces, Desalination 288 (2012) 126–134 (0).

[8] N. Ghaffour, T.M. Missimer, G.L. Amy, Technical review and evaluation of the economics of water desalination: current and future challenges for better water supply sustainability, Desalination 309 (2013) 197–207 (0).

[9] J.A. Bush, J. Vanneste, T.Y. Cath, Membrane distillation for concentration of hypersaline brines from the Great Salt Lake: effects of scaling and fouling on performance, efficiency, and salt rejection, Sep. Purif. Technol. 170 (2016) 78–91.

[10] H. Müller-Steinhagen, M. Malayeri, A. Watkinson, Heat exchanger fouling: mitigation and cleaning strategies, Heat Transfer Eng. 32 (3–4) (2011) 189–196.

[11] D. Hou, et al., Humic acid fouling mitigation by ultrasonic irradiation in membrane distillation process, Sep. Purif. Technol. 154 (2015) 328–337.

[12] K.D. Demadis, et al., Industrial water systems: problems, challenges and solutions for the process industries, Desalination 213 (1–3) (2007) 38–46.

[13] D. Lu, et al., Hydrophilic Fe$_2$O$_3$ dynamic membrane mitigating fouling of support ceramic membrane in ultrafiltration of oil/water emulsion, Sep. Purif. Technol. 165 (2016) 1–9.

[14] K.H. Teng, et al., Fouling mitigation on heat exchanger surfaces by EDTA-treated MWCNT-based water nanofluids, J. Taiwan Inst. Chem. Eng. 60 (2016) 445–452.

[15] Y. Pan, et al., DEM simulation and fractal analysis of particulate fouling on coal-fired utility boilers' heating surfaces, Powder Technol. 231 (2012) 70–76.

[16] K.H. Teng, et al., Mitigation of heat exchanger fouling in industry using catalytic materials, Desalin. Water Treat. (2015) 1–6.

[17] K. Palanisamy, V.K. Subramanian, CaCO$_3$ scale deposition on copper metal surface; effect of morphology, size and area of contact under the influence of EDTA, Powder Technol. 294 (2016) 221–225.

[18] B. Bansal, X.D. Chen, H. Müller-Steinhagen, Analysis of 'classical' deposition rate law for crystallisation fouling, Chem. Eng. Process. Process Intensif. 47 (8) (2008) 1201–1210.

[19] X. Zhao, X.D. Chen, A critical review of basic crystallography to salt crystallization fouling in heat exchangers, Heat Transfer Eng. 34 (8–9) (2012) 719–732.

[20] T.M. Pääkkönen, et al., Crystallization fouling of CaCO$_3$ – analysis of experimental thermal resistance and its uncertainty, Int. J. Heat Mass Transf. 55 (23–24) (2012) 6927–6937.

[21] S. Kazi, Fouling and Fouling Mitigation on Heat Exchanger Surfaces, INTECH Open Access Publisher, 2012.

[22] F. Rahman, Z. Amjad, 14 Scale Formation and Control in Thermal Desalination Systems, 2010.

[23] G. Qi, F. Jiang, Parametric study of particle distribution in tube bundle heat exchanger, Powder Technol. 271 (2015) 210–220.

[24] S.N. Kazi, G.G. Duffy, X.D. Chen, Mineral scale formation and mitigation on metals and a polymeric heat exchanger surface, Appl. Therm. Eng. 30 (14–15) (2010) 2236–2242.

[25] L.D. Tijing, et al., Mitigation of scaling in heat exchangers by physical water treatment using zinc and tourmaline, Appl. Therm. Eng. 31 (11 – 12) (2011) 2025–2031.

[26] J.W. Morse, R.S. Arvidson, A. Lüttge, Calcium carbonate formation and dissolution, Chem. Rev. 107 (2) (2007) 342–381.

[27] S. El Bécaye Maïga, et al., Heat transfer enhancement in turbulent tube flow using Al$_2$O$_3$ nanoparticle suspension, Int. J. Numer. Methods Heat Fluid Flow 16 (3) (2006) 275–292.

[28] F. Dittus, L. Boelter, Heat transfer in automobile radiators of the tubular type, Int. Commun. Heat Mass Transfer 12 (1) (1985) 3–22.

[29] B.C. Pak, Y.I. Cho, Hydrodynamic and heat transfer study of dispersed fluids with submicron metallic oxide particles, Exp. Heat Transfer Int. J. 11 (2) (1998) 151–170.

[30] V. Gnielinski, New equations for heat and mass transfer in the turbulent flow in pipes and channels, NASA STI/Recon Technical Report A, Vol. 75, 1975, p. 22028.

[31] L. Tijing, et al., Efficacy of zinc and tourmaline in mitigating corrosion of carbon steel in non-flow mode, Chem. Pap. 67 (10) (2013) 1304–1310.

[32] M.T.G. Ruelo, et al., Assessing the effect of catalytic materials on the scaling of carbon steel, Desalination 313 (2013) 189–198.

[33] S.N. Kazi, et al., Study of mineral fouling mitigation on heat exchanger surface, Desalination 367 (2015) 248–254 (0).

[34] M. Alahmad, Experimental study of scale formation in sea water environment, J. King Saud Univ. 17 (1) (2004) 73–88.

[35] Awad, M.M., et al., Effect of flow velocity on the surface fouling. Mansoura Eng. J. 32: p. M27-M37. **Q11**

[36] T.A. Hoang, M. Ang, A.L. Rohl, Effects of process parameters on gypsum scale formation in pipes, Chem. Eng. Technol. 34 (6) (2011) 1003–1009.

[37] K. Ceylan, G. Kelbaliyev, The roughness effects on friction and heat transfer in the fully developed turbulent flow in pipes, Appl. Therm. Eng. 23 (5) (2003) 557–570.

[38] P. Walker, R. Sheikholeslami, Assessment of the effect of velocity and residence time in CaSO$_4$ precipitating flow reaction, Chem. Eng. Sci. 58 (16) (2003) 3807–3816.

[39] M. Alahmad, Factors affecting scale formation in sea water environments – an experimental approach, Chem. Eng. Technol. 31 (1) (2008) 149–156.

[40] D.J. Kukulka, M. Devgun, Fluid temperature and velocity effect on fouling, Appl. Therm. Eng. 27 (16) (2007) 2732–2744.

[41] Q. Yang, et al., Investigation of induction period and morphology of CaCO$_3$ fouling on heated surface, Chem. Eng. Sci. 57 (6) (2002) 921–931.

[42] J.W. Mullin, 5 - nucleation, Crystallization, fourth ed.Butterworth-Heinemann, Oxford 2001, pp. 181–215.

[43] S. Kazi, G. Duffy, X. Chen, Fouling and fouling mitigation on heated metal surfaces, Desalination 288 (2012) 126–134.

[44] S.N. Kazi, G.G. Duffy, X.D. Chen, Fouling mitigation of heat exchangers with natural fibres, Appl. Therm. Eng. 50 (1) (2013) 1142–1148.

[45] K. Palanisamy, et al., A novel phenomenon of effect of metal on calcium carbonate scale, morphology, polymorphism and its deposition, Mater. Res. Innov. (2016) 1–10.

[46] S.P. Gopi, V. Subramanian, Polymorphism in CaCO$_3$—effect of temperature under the influence of EDTA (di sodium salt), Desalination 297 (2012) 38–47.

[47] J.W. Mullin, 6 - crystal growth, Crystallization, fourth ed.Butterworth-Heinemann, Oxford 2001, pp. 216–288.